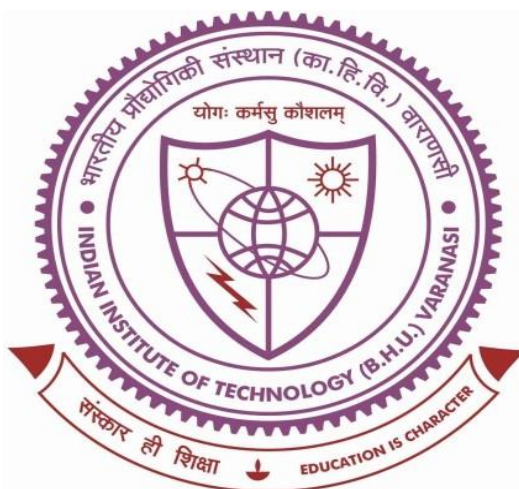


**Post-combustion CO₂ capture by using novel
BAE+DMAE, HMDA+DMAE and
TETA+DMAE aqueous amine blends**



Thesis submitted in partial fulfillment
for the award of degree

of

Doctor of Philosophy

By

Ashish Gautam

**Department of Chemical Engineering & Technology
Indian Institute of Technology
(Banaras Hindu University)
Varanasi – 221005, India**

Roll No. 19041007

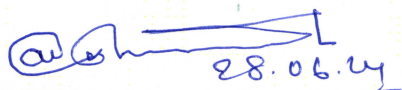
2024

*Dedicated to my beloved
Parents, &
Sisters, Ms. Archana &
Ms. Priyanka*

CERTIFICATE

It is certified that the work contained in this thesis entitled "**Post-combustion CO₂ capture by using novel BAE+DMAE, HMDA+DMAE and TETA+DMAE aqueous amine blends**" by **Ashish Gautam** has been carried out under my supervision, and it has not been submitted elsewhere for a degree.

It is further certified that **Ashish Gautam** has fulfilled all the requirements of comprehensive Examination, Candidacy, and SOTA for the award of Ph.D. Degree.


28.06.24

Prof. Monoj Kumar Mondal
(Supervisor)

Professor

Department of Chemical Engineering & Technology,

Indian Institute of Technology

(Banaras Hindu University)

Varanasi-221005,

Uttar Pradesh, India

प्राचार्य/Professor

रासायनिक अभियांत्रिकी एवं प्रौद्योगिकी विभाग

Deptt. of Chemical Engg. & Tech.

भारतीय प्रौद्योगिकी संस्थान

Indian Institute of Technology

काशी हिन्दू विश्वविद्यालय

Banaras Hindu University

वाराणसी/Varanasi-221005

DECLARATION BY THE CANDIDATE


I, **Ashish Gautam**, certify that the work embodied in this thesis is my own bonafide work and carried out by me under the supervision of **Prof. Monoj Kumar Mondal** from July 2019 to June 2024, at the **Department of Chemical Engineering & Technology**, Indian Institute of Technology (Banaras Hindu University) Varanasi. The matter embodied in this thesis has not been submitted for the award of any other degree/diploma. I declare that I have faithfully acknowledged and given credits to the research workers wherever their works have been cited in this thesis. I further declare that I have not willfully copied any other's work, paragraphs, text, data, results, etc., reported in the journal, books, magazines, reports, dissertations, thesis, etc., or available at websites and have not included them in this thesis and have not cited as my own work.

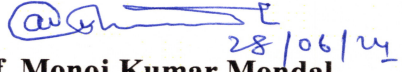
Date: 28/06/2024
Place: IIT (BHU), Varanasi

Ashish Gautam
(Ashish Gautam)

CERTIFICATE BY THE SUPERVISOR

It is certified that the above statement made by the student is correct to the best of my knowledge.


28.06.2024
Prof. Monoj Kumar Mondal
(Supervisor)


28/06/24
Prof. Monoj Kumar Mondal
(Head of Department)

Department of Chemical Engineering
& Technology,
Indian Institute of Technology
(Banaras Hindu University)
Varanasi-221005,
Uttar Pradesh, India
प्राचार्य/Professor

संसायनिक अभियांत्रिकी एवं प्रौद्योगिकी विभाग
Deptt. of Chemical Engg. & Tech.
भारतीय प्रौद्योगिकी संस्थान
Indian Institute of Technology
काशी हिन्दू विश्वविद्यालय
Banaras Hindu University
वाराणसी/Varanasi-221005

Department of Chemical Engineering
& Technology,
Indian Institute of Technology
(Banaras Hindu University)
Varanasi-221005,
Uttar Pradesh, India

iii
विभागाध्यक्ष/Head
संसायनिक अभियांत्रिकी एवं प्रौद्योगिकी विभाग
Deptt. of Chemical Engg. & Tech.
भारतीय प्रौद्योगिकी संस्थान/Indian Institute of Technology
काशी हिन्दू विश्वविद्यालय/Banaras Hindu University

COPY RIGHT TRANSFER CERTIFICATE

Title of the thesis: "Post-combustion CO₂ capture by using novel BAE+DMAE, HMDA+DMAE and TETA+DMAE aqueous amine blends".

Name of the student: Ashish Gautam

Copyright Transfer

The undersigned hereby assigns to the Indian Institute of Technology (Banaras Hindu University) Varanasi, Uttar Pradesh, India, all rights under the copyright that may exist in and for the above thesis submitted for the award of the "Doctor of Philosophy" degree.

Date: 28/06/2024
Place: IIT (BHU), Varanasi

Ashish Gautam
(Ashish Gautam)

Note: However, the author may reproduce or authorize others to reproduce material extracted verbatim from the thesis, or derivative of the thesis for the author's personal use, provided that the source and the Institute's copyright notice are indicated.

ACKNOWLEDGEMENT

I express my sincere gratitude to my respected supervisor **Prof. Monoj Kumar Mondal**, Department of Chemical Engineering & Technology, IIT (BHU) Varanasi, who has provided me with endless support, guidance, valuable suggestions, and motivation during the entire Ph.D. program. Working under his supervision is a new experience in the teaching and research field, which I can implement for human society in the near future. Sir has provided me with many essential research facilities, and under his valuable guidance, I have built up my confidence to showcase my inner potential for research. His thoughtful and valuable reviews, constructive criticism, and diligent review of all the manuscripts have significantly improved my work. In addition, he has always provided me with both direct and indirect support and encouragement. I am incredibly grateful to him for believing in me and in my research work.

I would like to thank **Dr. Manoj Kumar**, Department of Chemical Engineering & Technology, IIT (BHU) Varanasi and **Prof. Y.C. Sharma**, Department of Chemistry, IIT (BHU) Varanasi, for their constructive suggestions given during every research progress evaluation committee meeting. I would like to thank DPGC members and all faculty members of the Department of Chemical Engineering & Technology, IIT (BHU) Varanasi, for their valuable guidance. I would especially acknowledge **Dr. D.K. Panda**, Joint Director and Head (CME), National Council for Cement and Building Materials (NCCBM), Ballabgarh, for always encouraging and supporting for my wellbeings.

I express my heartfelt gratitude towards my lab staff, i.e., Mr. Arjun Prasad Gond (Senior Technical Superintendent), Mr. Rajesh Kumar (Junior Technical Superintendent), and Mr.

Lal Bahadur Ram (Senior Technician), Instrumental Analysis Laboratory, IIT (BHU) Varanasi, for helping me during experimental work.

I am thankful to my seniors, friends, and juniors who have helped me throughout this Ph.D. research work. I thank my seniors Dr. Shailesh Kumar, Dr. Diwakar Pandey, Dr. Anuj Kumar Prajapati, Dr. Goutam Kishore Gupta, Ms. Nidhi Agnihotri, and Mr. Mohit Kumar for their valuable guidance and support. I would especially like to thank Mr. Neeraj Kumar Yadav and Mr. Rakesh Kumar, who have supported, motivated, and encouraged me every time during the Ph.D. program. I thank my friends Mr. Veeresh Verma, Mr. Abhishek Anand, and Mr. Parmanand Maurya for their valuable support. The efforts of juniors are also highly appreciated; I thank Mr. Akhil Kumar Gupta, Mr. Sujit Pimple, Mr. Manish Pandey, Mr. Pushkar Diwakar, and Ms. Puja Kumari for their helping behavior.

I am so grateful to my family, who have supported me in challenging situations and motivated me to achieve various milestones in life; all the credit goes to my parents, **Mr. Ram Baboo** and **Mrs. Savitri Gautam**, who have sacrificed many things for me. I am grateful to my sisters, **Ms. Archana Gautam** and **Ms. Priyanka Gautam**, without their efforts, I would not have been able to pursue higher education.

I am deeply thankful to the Ministry of Human Resource Department (MHRD), Government of India, for providing financial support during the entire Ph.D. research work. Finally, I would like to thank the almighty and those who helped me directly or indirectly.

Date: 28/06/2024

Place: IIT (BHU), Varanasi

Ashish Gautam
(Ashish Gautam)

TABLE OF CONTENTS

Thesis Certificates	ii
Acknowledgements	v
Table of Contents	vii
List of Figures	xvii
List of Tables	xxix
Nomenclatures	xxxv
Preface	xli
Chapter 1 Introduction	1
1.1 CO ₂ Emissions, consequences and its solution	1
1.2 Sources of CO ₂	5
1.3 Various carbon-capturing techniques	6
1.3.1 Pre-combustion technique	7
1.3.2 Post-combustion technique	10
1.3.3 Oxy-combustion technique	12
1.3.4 Comparison in between various CO ₂ capture technologies for CCS	15
1.4 Various available CO ₂ capture methodologies	20
1.4.1 Absorption	23
1.4.1.1 Physical absorption	23
1.4.1.2 Chemical absorption	26
1.4.1.2.1 Amine solvent chemistry	28
1.4.1.2.1.1 The primary and secondary amines	30
1.4.1.2.1.1.1 Hindered amine	30
1.4.1.2.1.1.2 Tertiary amine	31

1.4.1.2.1.3	Cyclic amine	31
1.4.1.2.1.4	Ammonia solution	32
1.4.1.2.1.5	Salt solution	33
1.4.1.2.1.6	Various amine blends	34
1.4.1.2.1.7	CO ₂ absorption mechanism	36
1.4.2	Adsorption	37
1.4.2.1	Classification of adsorption	37
1.4.2.1.1	Physical adsorption	37
1.4.2.1.2	Chemical adsorption	38
1.4.2.2	Regeneration strategies	39
1.4.2.2.1	Pressure swing adsorption (PSA)	39
1.4.2.2.2	Temperature swing adsorption (TSA)	40
1.4.2.2.3	Electrical swing adsorption (ESA)	40
1.4.3	Membrane technology	41
1.4.3.1	Facilitated membrane separation	43
1.4.3.2	Non-facilitated membrane separation	43
1.4.3.3	Mixed-matrix membrane separation	44
1.4.3.4	Gas membrane contractor separation	45
1.4.4	Cryogenic separation	45
1.4.5	Microalgae process	46
1.5	Novel biphasic phase-changing solvents for CO ₂ capture	48
1.5.1	Advantages and disadvantages of biphasic solvents	52
1.5.2	Concept of lipophilic amine solvents	53
1.5.3	DMX TM process	55
1.5.4	Solvent screening and their selection	56

1.6	Research progress of biphasic amine solvents	58
1.6.1	Development of phase splitting-agent	58
1.6.2	Designing of the multistage phase separation process	60
1.7	Investigations performed by various researchers on biphasic solvents	62
	References	76
	Chapter 2 Literature Review and Objectives	95
2.1	Amine solvents for CO ₂ capture	95
2.2	Screening of tertiary amine for post-combustion CO ₂ capture	97
2.3	2-Dimethylaminoethanol (DMAE) tertiary amine for CO ₂ capture	107
2.4	Research gap / scope of the present work	115
2.5	Objective of the research work	116
	References	117
	Chapter 3 Novel aqueous amine blend of 2-(Butylamino)ethanol and 2-Dimethylaminoethanol for CO₂ capture: Equilibrium CO₂ loading, RSM optimization, desorption study, characterization and toxicity assessment	125
	Abstract	125
3.1	Introduction	126
3.2	Experimental section	132
3.2.1	Chemicals and instruments used	132
3.2.2	Analytical techniques for characterization	135
3.2.3	Description of the CO ₂ absorption setup	135
3.2.4	CO ₂ absorption experiment	137
3.2.5	Description and investigation of CO ₂ desorption setup	141
3.2.6	Heat duty and regeneration efficiency calculation	143
3.2.7	Study of heat of CO ₂ absorption (ΔH_{abs})	144

3.2.8	pH measurement of amine blend	145
3.2.9	Designing of experiments	146
3.2.10	Toxicity assessment	146
3.3	Reaction mechanism and characterization	148
3.3.1	Reaction chemistry of the amine blend system (BAE + DMAE + H ₂ O + CO ₂)	148
3.3.2	Fourier transform infrared spectroscopy (FTIR analysis)	150
3.3.3	Nuclear magnetic resonance spectroscopy (NMR analysis)	150
3.4	Results and discussion	151
3.4.1	Experimental setup validation	151
3.4.2	Equilibrium CO ₂ loading of the novel aqueous amine blend	153
3.4.2.1	Temperature effect on equilibrium CO ₂ loading for the BAE+DMAE novel aqueous amine blend	156
3.4.2.2	CO ₂ partial pressure effect on equilibrium CO ₂ loading for the BAE+DMAE novel aqueous amine blend	158
3.4.2.3	Activator's mole fraction effect on equilibrium CO ₂ loading for the BAE+DMAE novel aqueous amine blend	158
3.4.2.4	Solution concentration effect on equilibrium CO ₂ loading for the BAE+DMAE novel aqueous amine blend	160
3.4.2.5	Absorption time effect on equilibrium CO ₂ loading for the BAE+DMAE novel aqueous amine blend	161
3.4.3	Developing an empirical model for the novel aqueous amine blend of BAE+DMAE	161
3.4.4	Study of CO ₂ desorption results	163
3.4.5	Heat duty and regeneration efficiency investigation	165
3.4.6	Investigation on heat of CO ₂ absorption (ΔH_{abs})	167
3.4.7	Effect of pH on various amine blend samples	169

3.4.8	FTIR investigations	170
3.4.9	¹³ C NMR investigation of species in the novel aqueous amine blend	172
3.4.10	Study of toxicity level of BAE and DMAE	177
3.4.11	Optimization by using response surface methodology (RSM) – a statistical approach	179
3.4.11.1	RSM approach for establishing the correlation between factors and the final response	181
3.4.11.2	Empirical model validation through RSM software	186
3.4.11.3	Experimental runs validation by quadratic model	186
3.4.11.4	Investigation of ANOVA results	187
3.4.11.5	RSM modeling	190
3.4.11.6	Investigation on 3-D surfaces and contour graphs	193
3.4.11.7	Optimum value prediction and its validation by the RSM	199
3.5	Conclusions	204
	References	207
Chapter 4 Post-combustion CO₂ absorption-desorption performance of novel aqueous binary amine blend of Hexamethylenediamine (HMDA) and 2-Dimethylaminoethanol		221
	Abstract	221
4.1	Introduction	222
4.2	Experimental section	228
4.2.1	Chemicals and equipment	228
4.2.2	Experimental description of CO ₂ absorption setup	229
4.2.3	CO ₂ absorption experiments	229
4.2.4	Experimental setup validation	230
4.2.5	CO ₂ desorption setup description	232

4.2.6	pH measurement	232
4.2.7	Density measurement	232
4.2.8	^{13}C NMR characterization	233
4.2.9	FTIR characterization	234
4.2.10	Heat duty and regeneration efficiency	235
4.2.11	CO_2 absorption and desorption rate	236
4.2.12	Heat of CO_2 absorption (ΔH_{abs})	237
4.2.13	Designing of experimental runs by RSM software	238
4.2.14	Toxicity analysis	238
4.3	Chemical reactions of the novel amine blend system (HMDA + DMAE + H_2O + CO_2)	239
4.4	Results and discussion	242
4.4.1	Equilibrium CO_2 loading for the novel HMDA+DMAE amine blend	242
4.4.1.1	Effect of temperature on equilibrium CO_2 loading for novel aqueous HMDA+DMAE amine blend	243
4.4.1.2	Effect of CO_2 partial pressure on equilibrium CO_2 loading for novel aqueous HMDA+DMAE amine blend	246
4.4.1.3	Effect of mole fraction of HMDA on equilibrium CO_2 loading for novel aqueous HMDA+DMAE amine blend	247
4.4.1.4	Effect of solution concentration on equilibrium CO_2 loading for novel aqueous HMDA+DMAE amine blend	248
4.4.1.5	Effect of time on equilibrium CO_2 loading for novel aqueous HMDA+DMAE amine blend	249
4.4.2	An empirical model development for the novel aqueous amine blend of HMDA+DMAE	250
4.4.3	Investigation of CO_2 desorption results	252
4.4.4	Effect of CO_2 loading on pH	255

4.4.5	Thermophysical property: Density estimation	257
4.4.6	Study of ^{13}C NMR results	259
4.4.7	Study of FTIR results	262
4.4.8	Heat duty and regeneration efficiency results	263
4.4.9	Investigation of CO_2 absorption and desorption rates	266
4.4.10	Study of ΔH_{abs} results	270
4.4.11	Response surface methodology (RSM) – a statistical tool for optimization	272
4.4.11.1	Algorithm for implementing RSM for the novel HMDA+DMAE amine blend	272
4.4.11.2	RSM implementation in the present experimental work	273
4.4.11.3	Experimental investigation of RSM study	274
4.4.11.4	Establishing the relationship between the factors and the final response	275
4.4.11.5	Authentication of an empirical model by RSM-CCD approach	278
4.4.11.6	Selection of quadratic model and its authentication	278
4.4.11.7	Study of ANOVA results	279
4.4.11.8	Experimental modeling by RSM–CCD approach	282
4.4.11.9	Analysis of 3-D surfaces and contour graphs	285
4.4.11.10	Optimum value prediction and its validation by the RSM	291
4.4.12	Toxicity assessment for the novel amine blend	296
4.5	Conclusions	298
	References	301
Chapter 5 Post-combustion capture of CO_2 using novel aqueous Triethylenetetramine and 2-Dimethylaminoethanol amine blend: Equilibrium CO_2 loading-empirical model and optimization, CO_2 desorption, absorption heat, and ^{13}C NMR analysis		321

Abstract	321
5.1 Introduction	322
5.2 Materials and methods	325
5.2.1 Chemicals and equipment used	325
5.2.2 Description of the experimental setup	328
5.2.3 CO ₂ absorption investigation	328
5.2.4 CO ₂ desorption investigation	329
5.2.5 Heat of CO ₂ absorption (ΔH_{abs})	329
5.2.6 Response surface methodology (RSM) - statistical optimization approach	330
5.3 Reaction mechanism and its validation	330
5.3.1 Reaction chemistry of aqueous amine blend of TETA+DMAE+CO ₂ system	330
5.3.2 Nuclear magnetic resonance (NMR) spectroscopy	332
5.4 Results and discussion	332
5.4.1 Validation of the experimental setup	332
5.4.2 Equilibrium CO ₂ loading of the aqueous amine blend	333
5.4.2.1 Effect of mole fraction of activator (TETA) in the aqueous amine blend (TETA+DMAE) on equilibrium CO ₂ loading	336
5.4.2.2 Effect of total concentration of aqueous amine blend of TETA+DMAE on equilibrium CO ₂ loading	338
5.4.2.3 Effect of CO ₂ partial pressure on equilibrium CO ₂ loading	339
5.4.2.4 Effect of temperature on equilibrium CO ₂ loading for the aqueous amine blend of TETA+DMAE	339
5.4.3 Development of an empirical model for the TETA+DMAE aqueous amine blend	340
5.4.4 CO ₂ desorption analysis	341

5.4.5	Heat of CO ₂ absorption	346
5.4.6	¹³ C NMR spectral analysis	348
5.4.7	Response surface methodology (RSM) analysis	350
5.4.7.1	Development and analysis of equilibrium CO ₂ loading as a final response using response surface methodology	350
5.4.7.2	RSM generated model and its validation	353
5.4.7.3	Analysis of 3-D surfaces and contour graphs	357
5.4.7.4	Prediction of the optimum value and its verification by the RSM software	362
5.5	Conclusions	363
	References	365
	Chapter 6 Overall Conclusion and Future Recommendations	375
6.1	Overall conclusion	375
6.2	Future recommendations	377
	Appendix - A	379
	Appendix - B	391
	List of Publications	411

LIST OF FIGURES

<u>Figure No.</u>	<u>Caption</u>	<u>Page No.</u>
Figure 1.1	Flow diagram for CCS technique and its implementation [2,28,31]	2
Figure 1.2	Various CO ₂ capture techniques available for industrial purposes [2,28]	7
Figure 1.3	Schematic representation of the post-combustion technique [26,28,29]	11
Figure 1.4	A schematic representation of oxy-combustion technique for thermal power plant [2,32,49,51,54]	14
Figure 1.5	Commercialized statistics of CO ₂ capture techniques across the globe [2,23,132,133]	17
Figure 1.6	Proposed zero carbon emission power plant utilizing membrane technology [23,59]	42
Figure 1.7	Phase splitting behavior of amine solution by CO ₂ absorption [40,42,46]	50
Figure 2.1	Chemical structure of DMAE	107
Figure 3.1	The complete diagrammatic representation of the absorption setup used to perform absorption experiments for the novel aqueous amine blend of BAE+DMAE	139
Figure 3.2	The schematic representation of desorption setup used to perform desorption experiments for the novel aqueous amine blend of BAE+DMAE	142

-
-
- Figure 3.3** (a) Effect of temperature (T) on equilibrium CO_2 loading (α) for $C = 1 \text{ mol/L}$, 2 mol/L , and 3 mol/L at constant $P_{\text{CO}_2} = 20.27 \text{ kPa}$ and $m_{\text{BAE}} = 0.20$; (b) Effect of CO_2 partial pressure (P_{CO_2}) on equilibrium CO_2 loading (α) for $C = 1 \text{ mol/L}$, 2 mol/L , and 3 mol/L at constant $T = 313.15 \text{ K}$ and $m_{\text{BAE}} = 0.20$; (c) Effect of mole fraction of BAE (m_{BAE}) on equilibrium CO_2 loading (α) for $C = 1 \text{ mol/L}$, 2 mol/L , and 3 mol/L at constant $P_{\text{CO}_2} = 20.27 \text{ kPa}$ and $T = 313.15 \text{ K}$; (d) Effect of solution concentration (C) on equilibrium CO_2 loading (α) for $m_{\text{BAE}} = 0.05$, $m_{\text{BAE}} = 0.10$, $m_{\text{BAE}} = 0.15$, and $m_{\text{BAE}} = 0.20$ at constant $T = 313.15 \text{ K}$ and $P_{\text{CO}_2} = 20.27 \text{ kPa}$; (e) Effect of CO_2 loading time on equilibrium CO_2 loading (α) for $m_{\text{BAE}} = 0.05$, 0.10 , 0.15 , and 0.20 at constant $C = 1 \text{ mol/L}$, $T = 313.15 \text{ K}$, and $P_{\text{CO}_2} = 20.27 \text{ kPa}$; (f) Parity plot of experimental (α_{exp}) and calculated (α_{cal}) CO_2 loading (α) for the novel aqueous amine blend of BAE+DMAE
- Figure 3.4** Cyclic equilibrium CO_2 loading and cyclic capacity of 30 wt% MEA (i.e., 5 mol/L) for the novel aqueous amine blend of BAE+DMAE with $C = 1 \text{ mol/L}$, 2 mol/L , and 3 mol/L at constant $m_{\text{BAE}} = 0.20$
- Figure 3.5** The relationship between the heat duty and the solution concentration; (a) Comparison in between the heat duty values for 30 wt% MEA and the novel aqueous amine blend of BAE+DMAE for $C = 1 \text{ mol/L}$, 2 mol/L , and 3 mol/L ; (b) Effect of increasing BAE molar ratio in the aqueous solution of BAE+DMAE on heat duty

Figure 3.6	Plot of $\ln(P_{\text{CO}_2})$ vs. $(1/T)$ at different values of equilibrium CO_2 loading (i.e., $\alpha = 0.86$ and 0.90 mol CO_2/mol amine) for the determination of ΔH_{abs} for the novel aqueous amine blend of BAE+DMAE	168
Figure 3.7	FTIR analyses of species present in CO_2 -unloaded sample, CO_2 -loaded sample, and CO_2 -regenerated sample for the aqueous amine blend of BAE+DMAE	171
Figure 3.8	^{13}C NMR investigation of species present in aqueous amine blend of BAE+DMAE; (a) CO_2 -unloaded sample; (b) CO_2 -loaded sample; (c) CO_2 -regenerated sample	175
Figure 3.9	Value of toxicity represented in terms of lethal dose (LD_{50}) for various conventional amines	178
Figure 3.10	(a) Correlation between the predicted vs. actual values of equilibrium CO_2 loading as a final response; (b) Normal plot of residuals showing the relationship between the normal % probability vs. internally studentized residuals; (c) Correlation between the internally studentized residuals vs. predicted values of equilibrium CO_2 loading as a final response; (d) Relationship between the internally studentized residuals vs. the run number	192
Figure 3.11	(a) 3-D surface showing the effect of temperature (A) and CO_2 partial pressure (B) on final response; (b) Contour graph representing the effect of temperature (A) and CO_2 partial pressure (B) on final response; (c) 3-D surface showing the effect of temperature (A) and mole fraction of BAE (C) on final response; (d) Contour graph representing the effect of temperature (A) and mole fraction of BAE (C) on final response	194

-
-
- Figure 3.12** (a) 3-D surface showing the effect of temperature (A) and solution concentration (D) on final response; (b) Contour graph representing the effect of temperature (A) and solution concentration (D) on final response; (c) 3-D surface showing the effect of CO₂ partial pressure (B) and mole fraction of BAE (C) on final response; (d) Contour graph representing the effect of CO₂ partial pressure (B) and mole fraction of BAE (C) on final response 196
- Figure 3.13** (a) 3-D surface showing the effect of CO₂ partial pressure (B) and solution concentration (D) on final response; (b) Contour graph representing the effect of CO₂ partial pressure (B) and solution concentration (D) on final response; (c) 3-D surface showing the effect of mole fraction of BAE (C) and solution concentration (D) on final response; (d) Contour graph representing the effect of mole fraction of BAE (C) and solution concentration (D) on final response 198
- Figure 3.14** Desirability ramp, optimum values of factors and equilibrium CO₂ loading as a final response in numerical optimization 201
- Figure 4.1** (a) Effect of temperature (T) on equilibrium CO₂ loading (α) for C = 1, 2, and 3 mol/L at constant P_{CO₂} = 25.33 kPa and m_{HMDA} = 0.20; (b) Effect of CO₂ partial pressure (P_{CO₂}) on equilibrium CO₂ loading (α) for C = 1, 2, and 3 mol/L at constant T = 313.15 K and m_{HMDA} = 0.20; (c) Effect of mole fraction of HMDA (m_{HMDA}) on equilibrium CO₂ loading (α) for C = 1, 2, and 3 mol/L at constant P_{CO₂} = 20.27 kPa and T = 313.15 K; (d) Effect of solution concentration (C) on equilibrium CO₂ loading 245

- (α) for $m_{\text{HMDA}} = 0.05, 0.10, 0.15, 0.20$ at constant $T = 313.15$ K and $P_{\text{CO}_2} = 20.27$ kPa; (e) Effect of CO_2 loading time on equilibrium CO_2 loading (α) for $m_{\text{HMDA}} = 0.05, 0.10, 0.15,$ and 0.20 at constant $C = 1$ mol/L, $T = 313.15$ K, and $P_{\text{CO}_2} = 20.27$ kPa; (f) Parity plot of experimental (α_{exp}) and calculated (α_{cal}) CO_2 loading for the novel aqueous amine blend of HMDA+DMAE
- Figure 4.2** Cyclic equilibrium CO_2 loading ($\Delta\alpha$) and cyclic capacity for 30 wt% MEA and for solution concentrations, i.e., $C = 1, 2,$ and 3 mol/L at $T = 313.15$ K, $P_{\text{CO}_2} = 25.33$ kPa, and $m_{\text{HMDA}} = 0.20$ for the novel aqueous amine blend of HMDA+DMAE for post-combustion CO_2 capture 254
- Figure 4.3** Effect of solution concentration, i.e., $C = 1, 2,$ and 3 mol/L on solution pH for CO_2 -unloaded, CO_2 -loaded, and CO_2 -regenerated novel aqueous amine blend of HMDA+DMAE at $T = 313.15$ K, $P_{\text{CO}_2} = 25.33$ kPa, and $m_{\text{HMDA}} = 0.20$ 256
- Figure 4.4** The correlation between solution concentration and molar ratio of HMDA on heat duty; (a) comparison between the heat duty values for 30 wt% MEA and solution concentration, i.e., $C = 1, 2,$ and 3 mol/L for the novel aqueous amine blend of HMDA+DMAE for post-combustion CO_2 capture; (b) Effect of increasing the HMDA molar ratio in the novel aqueous amine blend of HMDA+DMAE on heat duty at $T = 313.15$ K, $P_{\text{CO}_2} = 25.33$ kPa, and $C = 3$ mol/L 264
- Figure 4.5** (a) Effect of increasing molar ratio of HMDA in the novel 268

- aqueous amine blend of HMDA+DMAE on the initial absorption rate; (b) Effect of increasing molar ratio of HMDA in the novel aqueous amine blend of HMDA+DMAE on the initial desorption rate
- Figure 4.6** Plot in between $\ln P_{\text{CO}_2}$ and $1/T$ for two different sets of equilibrium CO_2 loading i.e., $\alpha = 1.00$ and $\alpha = 1.07$ mol CO_2 /mol amine for the estimation of ΔH_{abs} for the novel aqueous amine blend of HMDA+DMAE for post-combustion CO_2 capture 271
- Figure 4.7** Plot of run points correlating factors with equilibrium CO_2 loading as a final response (Y): (a) Temperature (A) vs. Y; (b) CO_2 partial pressure (B) vs. Y; (c) Mole fraction of HMDA (C) vs. Y; (d) Solution concentration (D) vs. Y 277
- Figure 4.8** (a) The relationship between the actual vs. predicted values for the estimation of equilibrium CO_2 loading as a final response (Y) for the novel aqueous amine blend of HMDA+DMAE; (b) Normal plot of residuals establishing a relationship between the internally studentized residuals vs. normal % probability; (c) Relationship between the predicted values of the final response (Y) vs. internally studentized residuals; (d) Correlation between the run number vs. internally studentized residuals 284
- Figure 4.9** (a) 3-D surface representation of factors, i.e., temperature (A) and CO_2 partial pressure (B) and their effect on equilibrium CO_2 loading as a final response; (b) Contour graphical representation of factors, i.e., temperature (A) and CO_2 partial pressure (B) and their effect on equilibrium CO_2 loading as a 286

final response; (c) 3-D surface representation of factors, i.e., temperature (A) and mole fraction of HMDA (C) and their effect on equilibrium CO₂ loading as a final response; (d) Contour graphical representation of factors, i.e., temperature (A) and mole fraction of HMDA (C) and their effect on equilibrium CO₂ loading as a final response

Figure 4.10 (a) 3-D surface representation of factors, i.e., temperature (A) and solution concentration (D) and their effect on equilibrium CO₂ loading as a final response; (b) Contour graphical representation of factors, i.e., temperature (A) and solution concentration (D) and their effect on equilibrium CO₂ loading as a final response; (c) 3-D surface representation of factors, i.e., CO₂ partial pressure (B) and mole fraction of HMDA (C) and their effect on equilibrium CO₂ loading as a final response; (d) Contour graphical representation of factors, i.e., CO₂ partial pressure (B) and mole fraction of HMDA (C) and their effect on equilibrium CO₂ loading as a final response

Figure 4.11 (a) 3-D surface representation of factors, i.e., CO₂ partial pressure (B) and solution concentration (D) and their effect on equilibrium CO₂ loading as a final response; (b) Contour graphical representation of factors, i.e., CO₂ partial pressure (B) and solution concentration (D) and their effect on equilibrium CO₂ loading as a final response; (c) 3-D surface representation of factors, i.e., mole fraction of HMDA (C) and solution concentration (D) and their effect on equilibrium CO₂ loading as a final response; (d) Contour graphical representation of

	factors, i.e., mole fraction of HMDA (C) and solution concentration (D) and their effect on equilibrium CO ₂ loading as a final response	
Figure 4.12	Desirability ramp for numerical optimization of independent variables and equilibrium CO ₂ loading as a final response	293
Figure 4.13	Toxicity assessment in terms of LD ₅₀ values for various conventional amines	297
Figure 5.1	(a) Effect of mole fraction of TETA (m_{TETA}) on equilibrium CO ₂ loading (α) at constant $P_{\text{CO}_2} = 17.73$ kPa, $T = 315.65$ K, and at different $C = 1, 2,$ and 3 mol/L (b) Effect of total solution concentration (C) on equilibrium CO ₂ loading (α) at constant $P_{\text{CO}_2} = 17.73$ kPa, $T = 315.65$ K, and at different $m_{\text{TETA}} = 0.05, 0.13,$ and 0.2 (c) Effect of CO ₂ partial pressure (P_{CO_2}) on equilibrium CO ₂ loading (α) at constant $T = 315.65$ K, $m_{\text{TETA}} = 0.13,$ and at different $C = 1, 2,$ and 3 mol/L (d) Effect of temperature (T) on equilibrium CO ₂ loading (α) at constant $P_{\text{CO}_2} = 17.73$ kPa, $m_{\text{TETA}} = 0.13$ and at different $C = 1, 2,$ and 3 mol/L	337
Figure 5.2	Cyclic equilibrium CO ₂ loading and cyclic capacity of 30 wt% MEA solution and aqueous amine blend of TETA+DMAE with $m_{\text{TETA}} = 0.13$ at $C = 1$ mol/L, 2 mol/L and 3 mol/L	345
Figure 5.3	Plot of $\ln(P_{\text{CO}_2})$ vs. $(\frac{1}{T})$ at different equilibrium CO ₂ loading for estimating heat of absorption (ΔH_{abs}) for the aqueous amine blend of TETA+DMAE	347
Figure 5.4	¹³ C NMR analyses of aqueous amine blend of TETA+DMAE	349

- (a) before CO₂ loading (b) after CO₂ loading
- Figure 5.5** (a) The actual vs. predicted plot of equilibrium CO₂ loading as a final response (b) The plot of internally studentized residuals vs. normal percentage probability of equilibrium CO₂ loading (c) The predicted equilibrium CO₂ loading and internally studentized residuals plot (d) Internally studentized residuals versus the run number 356
- Figure 5.6** (a) 3-D surface representation of temperature (A), mole fraction of TETA (B), and equilibrium CO₂ loading (b) Contour plot showing the effect of temperature (A), mole fraction of TETA (B) on equilibrium CO₂ loading (c) 3-D surface representation of temperature (A), solution concentration (C), and equilibrium CO₂ loading (d) Contour plot showing the effect of temperature (A), solution concentration (C) on equilibrium CO₂ loading 358
- Figure 5.7** (a) 3-D surface representation of temperature (A), partial pressure of CO₂ (D), and equilibrium CO₂ loading (b) Contour plot showing the effect of temperature (A) and partial pressure of CO₂ (D) on equilibrium CO₂ loading (c) 3-D surface representation of mole fraction of TETA (B), solution concentration (C), equilibrium CO₂ loading (d) Contour plot showing the effect of mole fraction of TETA (B) and solution concentration (C) on equilibrium CO₂ loading 359
- Figure 5.8** (a) 3-D surface representation of mole fraction of TETA (B), partial pressure of CO₂ (D), and equilibrium CO₂ loading (b) Contour plot showing the effect of mole fraction of TETA (B) and partial pressure of CO₂ (D) on equilibrium CO₂ loading (c) 361

	3-D surface representation of solution concentration (C), partial pressure of CO ₂ (D), and equilibrium CO ₂ loading (d) Contour plot showing the effect of solution concentration (C) and partial pressure of CO ₂ (D) on equilibrium CO ₂ loading	
Figure A1	The principle of pre-combustion technique [28,23,49]	379
Figure A2	Complete process flow diagram of pre-combustion technique used in thermal power plant [23,32]	379
Figure A3	Classification of chemical solvents used in CO ₂ capture [30,37,57]	380
Figure A4	Industrial process representation of CO ₂ recovery through chemical absorption by post combustion technique [2,28,54,59,71]	381
Figure A5	Principle of gas separation by selective membrane [27,51]	382
Figure A6	Plot of run points correlating independent variable with equilibrium CO ₂ loading as a final response (a) Temperature (A) vs. equilibrium CO ₂ loading; (b) CO ₂ partial pressure (B) vs. equilibrium CO ₂ loading; (c) Mole fraction of BAE (C) vs. equilibrium CO ₂ loading; (d) Solution concentration (D) vs. equilibrium CO ₂ loading	383
Figure A7	¹³ C NMR investigation for the speciation analysis for the novel aqueous amine blend of HMDA+DMAE for the post-combustion CO ₂ capture; (a) CO ₂ -unloaded amine blend; (b) CO ₂ -loaded amine blend; (c) CO ₂ -regenerated amine blend	384
Figure A8	FTIR investigation of species present in CO ₂ -unloaded, CO ₂ -loaded and CO ₂ -regenerated solutions of novel aqueous amine blend of HMDA+DMAE for post-combustion CO ₂ capture	385

Figure A9	Step-by-step procedure for implementing the RSM by CCD for optimizing the equilibrium CO ₂ loading for the novel aqueous amine blend of HMDA+DMAE for post-combustion CO ₂ capture	386
Figure A10	Relationship of the equilibrium CO ₂ loading of the experimental data (α_{exp}) vs. calculated data (α_{cal}) [by Eq. 5.18]	387
Figure A11	Plot of run points correlating different independent variable: (a) temperature (A) vs. equilibrium CO ₂ loading (b) mole fraction of TETA (B) vs. equilibrium CO ₂ loading (c) solution concentration (C) vs. equilibrium CO ₂ loading (d) partial pressure of CO ₂ (D) vs. equilibrium CO ₂ loading	388
Figure A12	Ramp solutions with overall desirability of the independent variable and its final response	389

LIST OF TABLES

<u>Table No.</u>	<u>Caption</u>	<u>Page No.</u>
Table 1.1	Flue gas composition (in volume %) obtained from various CO ₂ capture techniques [26,29]	15
Table 1.2	Comparison in between various available CO ₂ capture technologies [2,23,24,26,28,54]	18
Table 1.3	The operating conditions along with the performance of carbon-capturing techniques [26,29,31,57,59]	19
Table 1.4	The operating conditions with the performance of various CO ₂ capture methodology [26,48,49,59]	21
Table 1.5	Common physical solvents, along with their general properties, are used to capture CO ₂ in pre-combustion technology [19,23,28,59]	25
Table 1.6	Physical characteristics with important properties of some selected chemical solvents [19]	29
Table 1.7	Examples of some lipophilic amines [30,38,43]	54
Table 1.8	Investigations conducted over the past 10 years on biphasic solvents by various researchers	69
Table 1.9	List of commercial CO ₂ capture projects under operation from 1972 to 2023 [130,132,133]	72
Table 2.1	Investigation conducted by various researchers for screening of tertiary amines for post-combustion CO ₂ capture	103

Table 2.2	Literature related to DMAE-based amine solvents for post-combustion CO ₂ capture	111
Table 3.1	Specification and entire properties of all the chemicals used in the experimental work	134
Table 3.2	Classification of different amines and their toxicity level based on LD ₅₀ range [49]	147
Table 3.3	Comparison between the equilibrium CO ₂ loading obtained from the literature and actual experiments performed for 30 wt% MEA under specified conditions of temperature and CO ₂ partial pressure ^a	152
Table 3.4	Experimental equilibrium CO ₂ loading (α_{exp}) and calculated equilibrium CO ₂ loading (α_{cal}) for the novel aqueous amine blend of BAE+DMAE under the specified operating condition at atmospheric pressure ^a	154
Table 3.5	Identification of chemical species present in the CO ₂ -unloaded, CO ₂ -loaded and CO ₂ -regenerated aqueous amine blend of BAE+DMAE	176
Table 3.6	Coded levels of all the independent variables used in the experiment of evaluating the equilibrium CO ₂ loading as a final response (Y) by using central composite design in the RSM software	183
Table 3.7	Values of experimental equilibrium CO ₂ loading as a final response (Y) and its predicted value for the runs created by the RSM software for the novel aqueous amine blend of BAE+DMAE under the specified operating condition at	184

	atmospheric pressure ^a	
Table 3.8	ANOVA analysis of quadratic model opted in CCD for the calculation of equilibrium CO ₂ loading as a final response	189
Table 3.9	Statistical parameters obtained from the analysis of variance (ANOVA) for the modelling of equilibrium CO ₂ loading as a final response	190
Table 3.10	Numerical solutions, goal, lower and upper limits of the factors to calculate the overall desirability of the system	200
Table 3.11	RSM predicted value vs. actual experimental value	203
Table 4.1	Validation of the experimental setup by comparing the values of equilibrium CO ₂ loading as determined by performing the actual experiments with the data obtained from the literature for 30 wt% MEA under particular operating conditions of temperature and CO ₂ partial pressure ^a	231
Table 4.2	Values of the unknown coefficients involved in the empirical modeling associated with the experimental data sets	251
Table 4.3	Statistical parameters involved in the ANOVA results for the modelling of equilibrium CO ₂ loading as a final response	281
Table 4.4	Numerical solutions, goal, lower and upper limits of the individual constraints in order to calculate the overall desirability of the system	292
Table 4.5	RSM predicted optimized result vs. actual experimental results	295
Table 5.1	Specification of chemicals, along with their significant properties used in this experimental work	327
Table 5.2	Experimental equilibrium CO ₂ loading (α_{exp}) and calculated	334

	equilibrium CO ₂ loading (α_{cal}) data of aqueous TETA+DMAE amine blend at different operating conditions such as CO ₂ partial pressure (P_{CO_2} , in kPa), mole fraction of TETA in the amine blend (m_{TETA}), total amine blend concentration (C , in mol/L), and temperature (T , in K) at atmospheric pressure ^a	
Table 5.3	Experimental runs generated by the response surface methodology (RSM) for the aqueous amine blend of TETA+DMAE and the equilibrium CO ₂ loading (Y) as a final response at different operating conditions (T , P_{CO_2} , m_{TETA} , C , and atmospheric pressure ^a)	343
Table 5.4	Experimental independent variables and their coded levels used for Central Composite design for the estimation of equilibrium CO ₂ loading as a final response	352
Table 5.5	ANOVA analysis of quadratic model in CCD for the estimation of equilibrium CO ₂	354
Table B1	US CO ₂ released in 2020 by some major industrial sectors [10]	391
Table B2	CO ₂ composition present in various process streams [49,59]	393
Table B3	Values of the unknown coefficients involved in the empirical modeling associated with the experimental data sets	393
Table B4	Values of the unknown coefficients involved in the empirical modeling associated with the RSM experimental data sets	394
Table B5	List of chemicals with their important specifications used in the entire experimental work	395

Table B6	Experimental equilibrium CO ₂ loading (α_{exp}) and empirical modeling calculated equilibrium CO ₂ loading (α_{cal}) for the novel aqueous amine blend of HMDA+DMAE under the specified operating conditions of T, P _{CO₂} , m _{HMDA} , and C working at an atmospheric pressure ^a	396
Table B9	Identification of intermediate species available in the CO ₂ -unloaded, CO ₂ -loaded and CO ₂ -regenerated aqueous amine blend of HMDA+DMAE in the ¹³ C NMR spectroscopy	399
Table B11	Coded levels of variables used to evaluate the final response (Y) by using RSM-CCD software-based technique	402
Table B12	Experimental equilibrium CO ₂ loading (α_{exp}), cook's distance, predictions calculated by RSM software and model calculated equilibrium CO ₂ loading (α_{cal}) for the novel aqueous amine blend of HMDA+DMAE under the specified operating conditions of T, P _{CO₂} , m _{HMDA} , and C working at an atmospheric pressure ^a	403
Table B13	Values of the unknown coefficients involved in the empirical modeling associated with the experimental run sets as generated by RSM-CCD approach	405
Table B14	ANOVA results for equilibrium CO ₂ loading for the novel aqueous amine blend of HMDA+DMAE	406
Table B15	Comparison of equilibrium CO ₂ loading data obtained from literatures and from experiments for 30 wt% aqueous MEA solution under specified temperature and pressure conditions, as well as relative deviation between experimental and	407

	literature data ^a	
Table B16	Values of unknown coefficients of the developed empirical model for separate experimental runs	407
Table B17	Identification of chemical species present in the amine blend before and after equilibrium CO ₂ loading	408
Table B18	Values of unknown coefficients of the developed empirical model for RSM generated experimental runs	409
Table B19	Statistical parameters obtained from the analysis of variance (ANOVA) for the model of equilibrium CO ₂ loading as a final response	409
Table B20	Numerical solutions, goal, lower and upper limits of the individual constraints in order to calculate the overall desirability of the system	410
Table B21	Results of RSM optimization based on the predicted value vs. actual experimental values	410

NOMENCLATURE

Abbreviations

% AARD	Percentage average absolute relative deviation
(CH ₃) ₄ Si	Tetramethylsilane
1DEA2P	1-Diethylamino-2-propanol
1DMA2P	1-Dimethylamino-2-propanol
2-PE	2-Piperidineethanol
2-PM	2-Piperidinemethanol
3DEA1P	3-Diethylamino-1-propanol
3DMA1P	3-Dimethylamino-1-propanol
4DEA-2B	4-Diethylamino-2-butanol
AEEA	2-((2-Aminoethyl)amino)ethanol
AMP	2-Amino-2-methyl-1-propanol
ANOVA	Analysis of variance
APPA	2-Amino-2-phenylpropionic acid
BAE	2-(Butylamino)ethanol
BBD	Box-behnken design
BDA	1,4-Butadiamine
CCD	Central composite design
CCS	Carbon capture and storage
CH _p A	Cycloheptylamine
CLC	Chemical looping combustion

COS	Carbonyl sulfide
DAB	1,4-Diaminobutane
DEA	Diethanolamine
DEEA	2-(Diethylamino)-ethanol
DEGDEE	Diethylene glycol diethyl ether
DETA	Diethylenetriamine
df	Degree of freedom
DIPA	Diisopropylamine
DMAE	2-Dimethylaminoethanol
DMBA	N, N-Dimethylbutylamine
DMCA	Dimethylcyclohexylamine
DMSO-d ₆	Dimethyl sulfoxide-d ₆
DPA	Di-n-propylamine
EAE	2-(Ethylamino)ethanol
EPA	Environmental protection agency
EPD	N-Ethylpiperidine
H _x A	Hexylamine
KE	Kent-Eisenberg
KF	Karl Fischer's method
MAPA	N-Methyl-1,3-diaminopropane
MCA	N-Methylcyclohexylamine
MDA	1,8-p-methanediamine
MDEA	Methyldiethanolamine

MEA	Monoethanolamine
MPD	N-Methylpiperidine
MSDS	Material safety data sheet
PA	Pipecolinic acid
PZ	Piperazine
RSM	Response surface methodology
SAPO	Silicoaluminophosphate
TBA	Tert-butylamine
TBA	Tributylamine
TBAE	2-(Ter-butylamino)ethanol
SBPA	N-Sec-Butyl-n-propylamine
TETA	Triethylenetetramine
TOU	2,5,7,10-Tetraoxaundecane
TPA	Tripropylamine
VLE	Vapor-liquid equilibrium

Symbols

ΔH_{abs}	Heat of CO ₂ absorption
C_{blend}	Amine blend's concentration
H_{CO_2}	Henry's constant
m_{BAE}	Mole fraction of BAE
m_{HMDA}	Mole fraction of HMDA
m_{TETA}	Mole fraction of TETA
n_{centre}	RSM's center point

P_{CO_2}	CO ₂ partial pressure
V_{CO_2}	Volume of CO ₂ gas released
α_{cal}	Calculated CO ₂ loading
α_{exp}	Experimental CO ₂ loading
α_{lit}	Literature available CO ₂ loading
τ_0	Constant coefficient
$\Delta\alpha$	Cyclic equilibrium CO ₂ loading
μ	Error function
A	Reactors surface area
C	Solution concentration
dT	Temperature difference
dX	Thickness
K	Thermal conductivity
LD ₅₀	Lethal dose value
N	Independent variables
N	Number of experiments
q	Steady state heat transfer
R	Universal gas constant
t	Desorption time
T	Temperature
Y	RSM's final response
α	CO ₂ loading
θ	Absorption time

Subscripts

cal	Calculated data
exp	Experimental data
lit	Literature data

PREFACE

The rapid increase in population leads to industrialization, afforestation, imbalance of energy demand, disturbance in natural habitats, soil/land degradation, and climate change. Various anthropogenic activities release harmful greenhouse gases in the atmosphere, which adversely pollute the environment. A large fraction of greenhouse gas is composed of carbon dioxide (CO₂), and its large emission is not favorable from an environmental point of view. Burning fossil fuels such as coal, natural gas, and oil is primarily responsible for the vast CO₂ emissions in the environment. Intergovernmental Panel on Climate Change (IPCC) has projected that if CO₂ emissions continue unchecked, the earth's temperature will rise by 2 °C by the year 2100. The anticipated data is horrifying since increasing CO₂ is responsible for increasing sea level, drought, flooding, storms, and other natural calamities. Therefore, it is necessary to capture CO₂ emitted from the flue gas.

Three main techniques are available for CO₂ capture: pre-combustion, post-combustion, and oxy-combustion. Among these techniques, post-combustion is the most mature way of CO₂ capturing; it has retrofitting properties with the existing units and its commercialization has also started. The post-combustion technique can be employed through different methodologies such as absorption, adsorption, membrane technology, cryogenic separation, and microalgae process. However, post-combustion CO₂ absorption by amine solvents is the well-established and most suitable method because of its high CO₂ capture recovery (80–95 %), low sensitive to acid gases, high mass transfer rate, and energy-intensive process. Monoethanolamine (MEA) is considered an industrial benchmark amine, but due to their disadvantages of high degradation, corrosive behavior, high vapor pressure, and costly regeneration process, researchers targeted different aqueous amine

blends to capture CO₂. Therefore, to overcome the challenges of the single amines, researchers are working on different amine blends to enhance the overall CO₂ absorption and desorption performance.

The least amount of research has been carried out in CO₂ capture through 2-Dimethylaminoethanol (DMAE), which is a novel tertiary amine and is considered an alternative to conventional Methyldiethanolamine (MDAE). When DMAE blended with some activators such as 2-(Butylamino)ethanol (BAE), Hexamethylenediamine (HMDA), and Triethylenetetramine (TETA) showed promising results. Therefore, the research objectives were decided to investigate the novel amine blends of BAE+DMAE, HMDA+DMAE, and TETA+DMAE for post-combustion CO₂ capture. The entire investigation of these novel amine blends has been incorporated in this thesis work, and they are summarized in separate chapters.

Chapter 1 describes the introduction of CO₂ emission, its global impacts, and its solution by using carbon capture and storage (CCS) technique. This chapter conducts an in-depth literature review on various CO₂ capture technologies and methodologies. Emerging biphasic amine solvents, their research progress, and various investigations conducted by different researchers on biphasic solvents are targeted.

Chapter 2 includes the literature review of screening of various tertiary amines for post-combustion CO₂ capture. Experimental investigations of CO₂ absorption and desorption have been targeted for screening purposes. Based on screening results, DMAE was selected, and previous experimental investigation on DMAE-based amine blends was deeply studied. Finally, the scope and objectives of the present work have been incorporated in this chapter.

Chapter 3 discusses the CO₂ absorption and desorption investigation by selecting the novel aqueous amine blend of 2-(Butylamino)ethanol (BAE) and 2-Dimethylaminoethanol (DMAE). In this work, equilibrium CO₂ loading was mainly targeted in the CO₂ absorption study, whereas cyclic capacity and cyclic equilibrium CO₂ loading were focused in the CO₂ desorption investigation. Reaction mechanism, ¹³C NMR and FTIR characterization, pH estimation, toxicity, heat of CO₂ absorption (ΔH_{abs}), and optimization were the prime objectives of the research work.

Chapter 4 explains the CO₂ absorption-desorption performance of a novel aqueous binary amine blend of Hexamethylenediamine (HMDA) and 2-Dimethylaminoethanol (DMAE). CO₂ absorption and desorption rate, heat duty and regeneration efficiency, thermophysical property, i.e., density estimation, etc., were the important parameters that were estimated to evaluate the performance of the novel chosen amine blend for post-combustion CO₂ capture.

Chapter 5 describes the selection of a novel aqueous Triethylenetetramine (TETA) and 2-Dimethylaminoethanol (DMAE) amine blend for post-combustion CO₂ capture. Equilibrium CO₂ loading was estimated and the results were validated by empirical modeling. The effect of process parameters on equilibrium CO₂ loading was determined for the chosen operating conditions. The entire reaction mechanism of the novel amine blend has been suggested, and ¹³C NMR characterization authenticated the same. At last, response surface methodology (RSM) was used to optimize the equilibrium CO₂ loading.

Chapter 6 summarizes the overall conclusion of the present research work and based on current investigation, future recommendations have been suggested.